Lack of bipolar see-saw in response to Southern Ocean wind reduction

A. Levermann,[1] J. Schewe,[1] and M. Montoya[2]

Received 3 April 2007; revised 16 May 2007; accepted 29 May 2007; published 28 June 2007.

[1] A cessation of the Atlantic meridional overturning circulation (AMOC) significantly reduces northward oceanic heat transport. In response to anomalous freshwater flux, this leads to the classic 'bipolar see-saw' pattern of northern cooling and southern warming in surface air and ocean temperatures. By contrast, as shown here in a coupled climate model, both northern and southern cooling are observed for an AMOC reduction in response to reduced wind stress in the Southern Ocean (SO). For very weak SO wind stress, not only the overturning circulation collapses, but sea ice export from the SO is strongly reduced. Consequently, sea ice extent and albedo increase in this region. The resulting cooling overcompensates the warming by the reduced northward heat transport. The effect depends continuously on changes in wind stress and is reversed for increased winds. It may have consequences for abrupt climate change, the last deglaciation and climate sensitivity to increasing atmospheric CO_2 concentration.
Citation: Levermann, A., J. Schewe, and M. Montoya (2007), Lack of bipolar see-saw in response to Southern Ocean wind reduction, *Geophys. Res. Lett.*, *34*, L12711, doi:10.1029/2007GL030255.

1. Introduction

[2] The northward heat transport by the Atlantic meridional overturning circulation (AMOC) [*Ganachaud and Wunsch*, 2000; *Talley*, 2003] has important consequences for global climate [*Zickfeld et al.*, 2007; *Vellinga and Wood*, 2007]. Presently, it favors mild northern European surface air temperature (SAT) and a northward excursion of the Intertropical Convergence Zone in the Atlantic sector [*Vellinga and Wood*, 2002]. An AMOC collapse significantly reduces the northward heat transport and yields a net heat transport to the Southern Hemisphere. Without any other processes involved this induces a time-delayed positive temperature anomaly in the south and therewith the so-called bipolar see-saw pattern of northern cooling and southern warming [*Crowley*, 1992].

[3] For the last glacial period abrupt climatic events (Dansgaard-Oeschger events) can be observed in Greenland ice cores [*North Greenland Ice Core Project members*, 2004]. These are accompanied by temperature variations recorded in Antarctic cores with Antarctica generally warming during a cold (stadial) phase in Greenland [*EPICA-Project*, 2006]. A possible dynamical explanation is associated with an abrupt reorganization of the AMOC in response to fluctuations in surface freshwater fluxes to the North Atlantic [*Ganopolski and Rahmstorf*, 2001]. In this theory, the time-delayed bipolar see-saw effect explains the characteristic temperature responses in the Northern and Southern Hemispheres. The temporal lead of the Northern Hemisphere can however not be inferred from paleodata [*Steig and Alley*, 2002]. An alternative view is that perturbations are induced from the SO and reach the North Atlantic with some time delay [e.g., *Blunier et al.*, 1998; *Weaver et al.*, 2003]. In order to reproduce the temporal sequence recorded in Greenland and Antarctic ice cores that would require a warming in the SO to be associated with a warming in the North Atlantic. The mechanism presented here yields such a lack of bipolar see-saw through perturbations in SO wind stress.

[4] The importance of SO winds for the deep AMOC is still a matter of intense investigation [*Kuhlbrodt et al.*, 2007]. *Toggweiler and Samuels* [1995] proposed that surface wind stress in the SO drives the AMOC and therefore influences its strength, while other studies emphasize the role of the thermohaline component of the circulation [e.g., *Rahmstorf and England*, 1997]. For the last glacial period, reconstructions of wind stress are presently not well constrained [*Crowley and North*, 1991; *Wunsch*, 2003, and references therein]. *Toggweiler et al.* [2006] argue that mid-latitude westerly winds are generally shifted equatorward during glacial periods. In combination with associated changes in SO overturning circulation and the carbon cycle, they suggest a positive feedback as an explanation for the observed Antarctic warming during the last deglaciation. The effect presented here in the global coupled climate model CLIM*BER*-3α yields such a warming for increased wind stress in the SO and could therefore augment their mechanism.

[5] The main novelty of our simulations is based on the fact that the AMOC in CLIM*BER*-3α is driven by SO winds with almost no upwelling in the Atlantic and Pacific basin [*Mignot et al.*, 2006] which is supported by observations but not reproduced by most state-of-the-art climate models. Potential implications for future climate change become apparent as recent model simulations, performed for the Fourth Assessment Report of the Intergovernmental Panel on Climate Change [*Meehl et al.*, 2007], suggest a strengthening of surface wind stress in response to atmospheric CO_2 increase under the A2 SRES scenario [*Fyfe and Saenko*, 2006]. In combination with our results this would lead to a global warming of about 0.15 K and hence contribute to climate sensitivity.

2. Model and Experiments

[6] The global coupled climate model CLIM*BER*-3α [*Montoya et al.*, 2005] combines a three-dimensional ocean general circulation model based on the GFDL MOM-3 code

[1] Earth System Analysis, Potsdam Institute for Climate Impact Research, Potsdam, Germany.
[2] Departamento Astrofísica y Ciencias de la Atmósfera, Universidad Complutense, Madrid, Spain.

0094-8276/07/2007GL030255$05.00

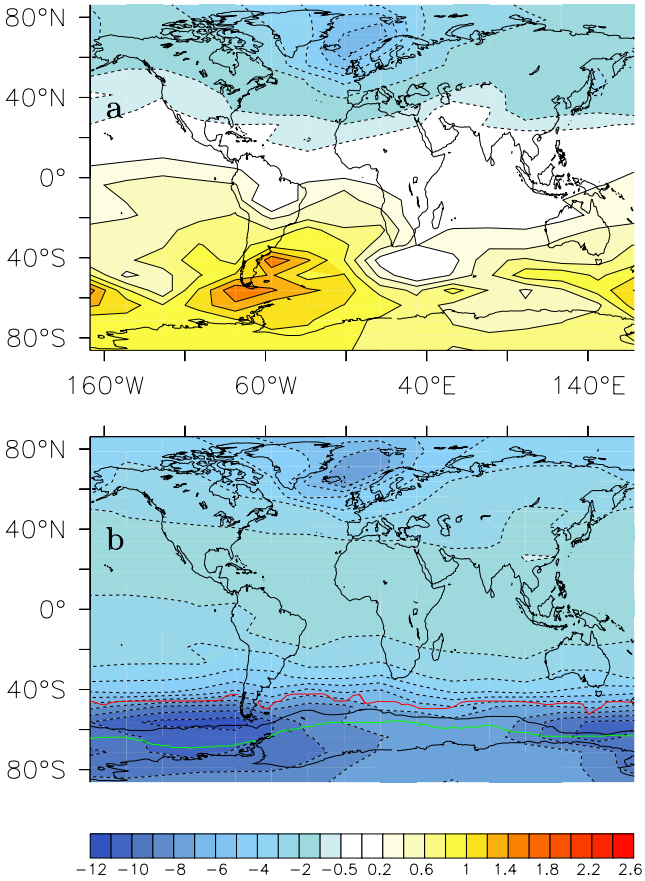

Figure 1. Annual SAT difference (in K, on- minus off-state): AMOC cessation is obtained by (a) application of 0.35 Sv of anomalous freshwater flux (FWF) to the northern North Atlantic (b) reduction in SO wind stress ($\alpha = 0.01$). Note the asymmetric color scale. The thick contours in the Southern Ocean in Figure 1b mark the level of 70% average winter sea ice cover for normal wind conditions ($\alpha = 1$, black), for collapsed AMOC ($\alpha = 0.01$, red), and for pre-industrial climate reconstructions [*Rayner et al.*, 2003] (year 1870, green).

[*Pacanowski and Griffies*, 1999] with a statistical-dynamical atmosphere model [*Petoukhov et al.*, 2000] and a dynamic and thermodynamic sea-ice model [*Fichefet and Morales Maqueda*, 1997]. The oceanic horizontal resolution is $3.75° \times 3.75°$ with 24 variably spaced vertical levels. In order to reduce numerical diffusion a second order moment tracer advection scheme is applied [*Prather*, 1986; *Hofmann and Morales Maqueda*, 2006]. Since we use a very low vertical diffusivity coefficient (10^{-5} m^2/s), the mixing induced upwelling both in the Atlantic and Pacific is small [*Mignot et al.*, 2006] and the AMOC is almost entirely driven by SO wind stress divergence through the so-called Drake Passage Effect [*Toggweiler and Samuels*, 1995].

[7] For the present study, oceanic wind stress is prescribed to the NCEP-NCAR reanalysis $\tau^0(x, y)$ [*Kistler et al.*, 2001]. We performed a series of experiments, in which the zonal oceanic wind stress component τ_x is multiplied with a factor α between 71.25°S and 30°S with $\alpha = 0.01$, 0.1, 0.2, 0.5, 1.0, 1.5 and 2.0. The simulations thus span a range of both reduced and enhanced surface forcing. Since the meridional distribution of τ_x, in the aforementioned latitudinal interval, has a quasi-sinusoidal shape (being close-to-zero at 71.25°S and 30°S, and maximum at about 51°S), this implies a modulation of both the wind stress magnitude, τ_x, and the wind stress gradient. In particular, in the latitude band of Drake Passage, between 62°S and 56°S, the maximum of the zonally averaged wind stress gradient, $T_y \equiv \partial_y \tau_x$, varies from $0.6 \cdot 10^{-8}$ N/m^3 in the $\alpha = 0.01$ experiment, to $34.1 \cdot 10^{-8}$ N/m^3 in the $\alpha = 2$ experiment. For each experiment, the model was run for several thousand years until an equilibrium state was reached. For comparison a simulation with 0.35 *Sv* = $0.35 \cdot 10^6$ m^3/s of enhanced freshwater flux to the North Atlantic (from 52°N to 80°N and from 48°W to 15°E) was carried out, leading to a collapse of the AMOC (experiment FWF, following [*Levermann et al.*, 2005]). This experiment was run for more than 5000 years with anomalous freshwater flux and prescribed NCEP/NCAR winds stress forcing.

3. Temperature Response to SO Wind Changes

[8] In experiments with enhanced freshwater flux into the North Atlantic such as the FWF experiment [*Manabe and Stouffer*, 1995; *Stouffer et al.*, 2006], surface air and ocean temperatures are found to cool in the Northern Hemisphere, and warm in the Southern Hemisphere as the AMOC is reduced (Figure 1a). This aforementioned bipolar see-saw pattern of opposite surface temperature changes originates from a reduction in northward oceanic heat transport associated with the AMOC.

[9] In CLIM*BER*-3α a similar AMOC reduction is obtained for near-zero SO wind stress (Figure 2a). However, these experiments do not exhibit the bipolar see-saw pattern. Instead, SAT cools in both hemispheres when the AMOC is reduced (Figure 1b). The effect does not show abrupt changes but depends continuously on SO wind stress gradient (Figure 2c). All experiments with $\alpha < 1$ exhibit global cooling relative to the standard simulation, while a slight global warming is observed for increased T_y. The same behavior is found for sea surface temperature while subsurface temperatures in the SO increase for weakened T_y due to reduced AMOC and thereby northward oceanic heat transport (not shown). Note that the negative surface temperature anomaly does not arise from reduced SO upwelling, since temperatures decrease with depth in this region. Due to reduced wind-driven outcropping of isopycnals and reduced brine rejection, convection is strongly reduced in the SO for weak wind stress. This could, in principle, lead to a local cooling as observed in response to anomalous freshwater forcing in the North Atlantic. However, the global cooling seen in Figure 1b and the corresponding sea surface temperature pattern can not be caused by a redistribution of heat within the ocean. A net heat loss of the lower troposphere is necessary and thus surface processes have to be responsible.

4. Sea Ice Mechanism

[10] The absence of a bipolar see-saw in our experiments is due to changes in sea ice cover and thereby altered albedo and atmosphere-ocean heat exchange in the SO. The south-

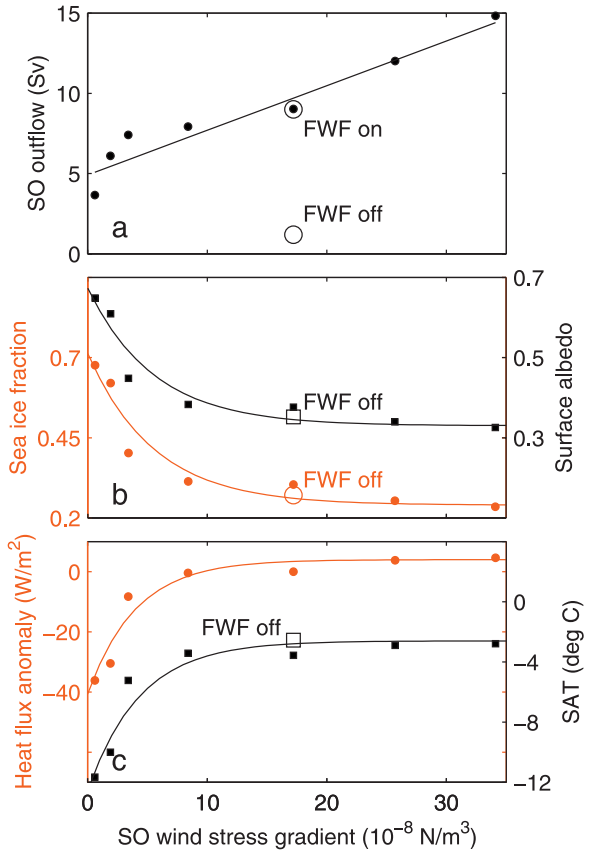

Figure 2. Changes with varying SO winds. (a) SO outflow (at 33.75°S). The line gives a linear approximation. For comparison, the AMOC on- and off-states of the anomalous freshwater flux (FWF) experiments are indicated by open circles. (b) Sea ice fraction (red dots) and surface albedo (black squares), averaged south of 40°S. Sea ice fraction increases as wind stress is reduced, enhancing surface albedo. The lines give exponential approximations with saturation at 0.24 and 0.33 for the sea ice fraction and surface albedo, respectively, as $T_y \rightarrow \infty$. (c) Ocean-atmosphere heat flux anomalies (red dots) and SAT (black squares), averaged south of 40°S. For decreasing wind stress, reduced heat flux into the atmospheric surface layer reduces surface temperature. The lines gives exponential approximations with saturation at 4 W/m^2 and −2.6°C for heat flux anomaly and for SAT, respectively, as $T_y \rightarrow \infty$. In Figures 2b and 2c, for sea ice fraction, albedo, and SAT, the AMOC off-states-values of the FWF experiment are given for comparison. FWF-on-state-values are equivalent to the $\alpha = 1$ experiment. See Figure 4 for a decomposition of the ocean-atmosphere heat flux into its radiative and turbulent components. The x-axis shows the maximum of the zonally averaged wind stress gradient T_y between 63.75°S and 52.5°S.

ern subpolar westerlies induce a northeastward Ekman sea ice transport. A reduction in SO surface wind stress consequently reduces northward sea ice export from the Antarctic region (Figure 3). As a result sea ice cover increases in the SO. The thick contours in Figure 1b indicate the 70%-winter-sea-ice-cover. The standard simulation ($\alpha = 1$, black) overestimates sea ice extent slightly compared to pre-industrial reconstructions (green) [*Rayner et al.*, 2003]. For smaller T_y, the 70%-sea-ice-margin is shifted northward by up to ∼15 degrees for $\alpha = 0.01$ (red) compared to standard conditions. The sea ice fraction south of 40°S (Figure 2b, red) increases from ∼30% with standard wind stress up to 70% for $\alpha = 0.01$. For enhanced wind stress sea ice cover declines and saturates around 24% (obtained from the red exponential curve in Figure 2b).

[11] Increased sea ice cover enhances surface albedo (Figure 2c) and insulates the ocean from the atmosphere. Both effects tend to cool the ocean surface in different ways. The increased albedo leads to a reduction of the absorption of incoming solar radiation at the surface. The effect is largest in Southern Hemisphere summer, when the incoming solar radiation is largest (Figure 4a), while in the Southern Hemisphere winter short wave radiative heat flux is near zero at the relevant latitudes. The insulation effect tends to reduce turbulent heat flux throughout the year (Figure 4b) but is strongest during the southern hemispheric winter when the ocean is much warmer than the atmosphere. Thus, the enhanced sea ice cover results in a reduction of the total amount of heat received by the atmosphere throughout the year (Figure 2c, red circles) and consequently yields an SAT reduction for low SO wind stress (Figure 2c, black squares).

5. Discussion and Conclusion

[12] In contrast to the classic bipolar see-saw pattern, we observe a cooling in both hemispheres for an AMOC weakening in response to a reduction in SO wind stress. This effect is explained by increased sea ice cover in the SO due to reduced sea ice export into warmer northern latitudes. This increases surface albedo and insulates the atmosphere from the ocean. Thus both radiative and turbulent heat loss over the SO are enhanced, which overcompensates the net heat gain due to reduced northward oceanic heat transport by the AMOC weakening. The latter effect is nevertheless found in subsurface.

[13] Albedo and insulation effect might be overestimated in CLIM*BER*-3α due to the larger SO sea ice extent in the standard simulation compared to pre-industrial reconstructions. On the other hand, changes in turbulent heat exchange might be underestimated because they are increasing with wind speed but are not affected by the changes in wind-

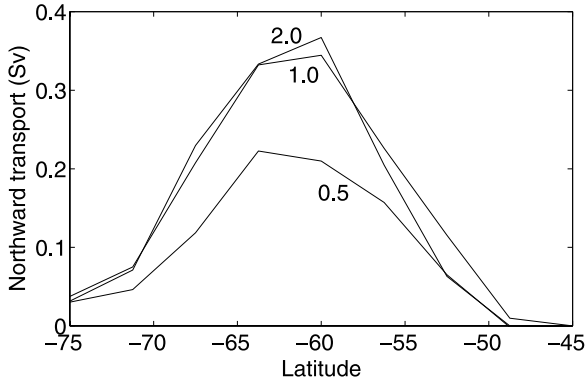

Figure 3. Zonally integrated annual mean northward sea ice transport (Sv) for $\alpha = 0.5$, 1.0, and 2.0.

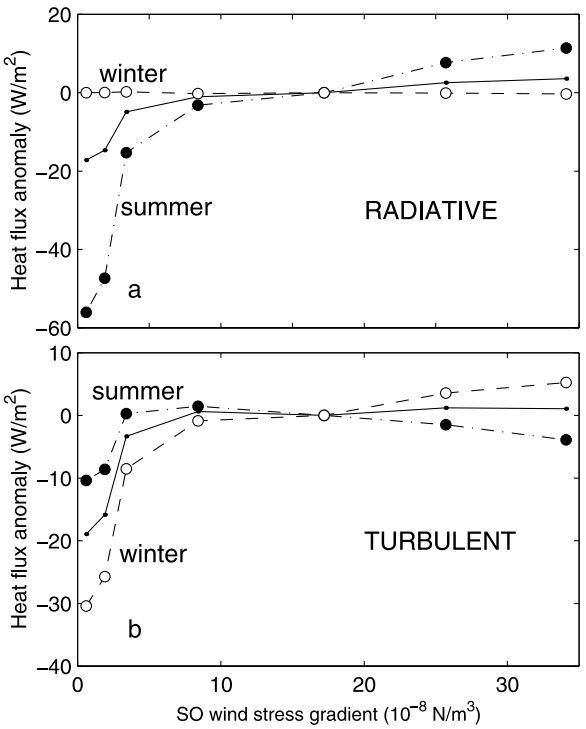

Figure 4. Changes of (a) radiative and (b) turbulent ocean-atmosphere heat flux in response to changed SO winds. Averages for Southern Hemisphere winter (June–August) are given by open circles and dashed lines, and for Southern Hemisphere summer (December–February) by dots and dotted lines. Solid lines give annual means. The effect of sea ice albedo on radiative heat uptake plays a role only in summer when there is significant insolation at high southern latitudes. The insulating effect of sea ice on turbulent heat exchange is largest in winter but occurs throughout the year.

stress that were prescribed in our experiments. The enhancement of turbulent heat flux with increasing wind speed would enhance the effect described here. In any case, the qualitative behaviour is quite straightforward and should be at play whenever wind stress changes in the SO.

[14] Recently, *Fyfe and Saenko* [2006] showed that SO winds increase in AOGCM projections of future climate change by 25% until 2100 under the A2 scenario. Their results indicated that an increase in SO winds by 20% for a doubling of atmospheric CO_2 concentration from 280 ppm to 560 ppm is in the realm of possibilities. In our model this would correspond to a global warming of about 0.15 K - a small but not negligible contribution to climate sensitivity.

[15] As mentioned in the introduction, further implications might arise for abrupt climatic events during the last glacial period and deglaciation. If these events were indeed triggered from the SO as opposed to the North Atlantic, a lack of the bipolar see-saw pattern might be necessary to explain the temporal evolution of events seen in the ice cores. The main result of our study, however, is that modifications in AMOC strength are not necessarily associated with a bipolar SAT and sea surface temperature response. AMOC changes due to SO wind stress variations can be associated with equal-sign temperature changes in both hemispheres.

[16] **Acknowledgments.** We are grateful to J. R. Toggweiler and J. Mignot for useful comments on the manuscript. A.L. was funded by the Gary Comer foundation, M.M. by the Ramón y Cajal Program and project CGL2005-06097/CLI of the Spanish Ministry for Science and Education.

References

Blunier, T., et al. (1998), Asynchrony of Antarctic and Greenland climate change during the last glacial period, *Nature*, *394*, 739–743.

Crowley, T. J. (1992), North Atlantic Deep Water cools the Southern Hemisphere, *Paleoceanography*, *7*, 489–497.

Crowley, T. J., and G. R. North (1991), *Paleoclimatology*, 349 pp., Oxford Univ. Press, Oxford, U. K.

EPICA-Project (2006), Eight glacial cycles from an Antarctic ice core, *Nature*, *444*, 195–198.

Fichefet, T., and M. A. Morales Maqueda (1997), Sensitivity of a global sea ice model to the treatment of ice thermodynamics and dynamics, *J. Geophys. Res.*, *102*, 12,609–12,646.

Fyfe, J. C., and O. A. Saenko (2006), Simulated changes in the extratropical Southern Hemisphere winds and currents, *Geophys. Res. Lett.*, *33*, L06701, doi:10.1029/2005GL025332.

Ganachaud, A., and C. Wunsch (2000), Improved estimates of global ocean circulation, heat transport and mixing from hydrographic data, *Nature*, *408*, 453–457.

Ganopolski, A., and S. Rahmstorf (2001), Rapid changes of glacial climate simulated in a coupled climate model, *Nature*, *409*, 153–158.

Hofmann, M., and M. A. Morales Maqueda (2006), Performance of a second-order moments advection scheme in an Ocean General Circulation Model, *J. Geophys. Res.*, *111*, C05006, doi:10.1029/2005JC003279.

Kistler, R., et al. (2001), The NCEP-NCAR 50-year reanalysis: Monthly means CD-ROM and documentation, *Bull. Am. Meteorol. Soc.*, *82*, 247–267.

Kuhlbrodt, T., A. Griesel, M. Montoya, A. Levermann, M. Hofmann, and S. Rahmstorf (2007), On the driving processes of the Atlantic meridional overturning circulation, *Rev. Geophys.*, *45*, RG2001, doi:10.1029/2004RG000166.

Levermann, A., A. Griesel, M. Hofmann, M. Montoya, and S. Rahmstorf (2005), Dynamic sea level changes following changes in the thermohaline circulation, *Clim. Dyn.*, *24*, 347–354.

Manabe, S., and R. J. Stouffer (1995), Simulation of abrupt climate change induced by freshwater input to the North Atlantic Ocean, *Nature*, *378*, 165–167.

Meehl, G. A., et al. (2007), Global climate projections, in *Climate Change 2007: The Physical Science Basis: Contribution of Working Group I to the Fourth Assessment Report of the Intergovernmental Panel on Climate Change*, Cambridge Univ. Press, New York, in press.

Mignot, J., A. Levermann, and A. Griesel (2006), A decomposition of the Atlantic meridional overturning circulation into physical components using its sensitivity to vertical diffusivity, *J. Phys. Oceanogr.*, *36*, 636–650.

Montoya, M., A. Griesel, A. Levermann, J. Mignot, M. Hofmann, A. Ganopolski, and S. Rahmstorf (2005), The Earth system model of intermediate complexity CLIM*BER*-3α. part I: Description and performance for present day conditions, *Clim. Dyn.*, *25*, 237–263.

North Greenland Ice Core Project members (2004), High-resolution record of Northern Hemisphere climate extending into the last glacial period, *Nature*, *431*, 147–151.

Pacanowski, R. C., and S. M. Griffies (1999), The MOM-3 manual, *Tech. Rep. 4*, NOAA Geophys. Fluid Dyn. Lab., Princeton, N. J.

Petoukhov, V., A. Ganopolski, V. Brovkin, M. Claussen, A. Eliseev, C. Kubatzki, and S. Rahmstorf (2000), CLIMBER-2: A climate system model of intermediate complexity. part I: Model description and performance for present climate, *Clim. Dyn.*, *16*, 1–17.

Prather, M. J. (1986), Numerical advection by conservation of second-order moments, *J. Geophys. Res.*, *91*, 6671–6681.

Rahmstorf, S., and M. H. England (1997), Influence of Southern Hemisphere winds on North Atlantic Deep Water flow, *J. Phys. Oceanogr.*, *27*, 2040–2054.

Rayner, N. A., D. E. Parker, E. B. Horton, C. K. Folland, L. V. Alexander, D. P. Rowell, E. C. Kent, and A. Kaplan (2003), Global analyses of sea surface temperature, sea ice, and night marine air temperature since the late nineteenth century, *J. Geophys. Res.*, *108*(D14), 4407, doi:10.1029/2002JD002670.

Steig, E. J., and R. B. Alley (2002), Phase relationship between Antarctic and Greenland climate records, *Ann. Glaciol.*, *35*, 451–456.

Stouffer, R. J., et al. (2006), Investigating the causes of the response of the thermohaline circulation to past and future climate changes, *J. Clim.*, *19*, 1365–1387.

Talley, L. D. (2003), Shallow, intermediate, and deep overturning components of the global heat budget, *J. Phys. Oceanogr.*, *33*, 530–560.

Toggweiler, J. R., and B. Samuels (1995), Effect of Drake Passage on the global thermohaline circulation, *Deep Sea Res., Part I*, *42*, 477–500.

Toggweiler, J. R., J. L. Russell, and S. R. Carson (2006), Midlatitude westerlies, atmospheric CO_2, and climate change during the ice ages, *Paleoceanography*, *21*, PA2005, doi:10.1029/2005PA001154.

Vellinga, M., and R. A. Wood (2002), Global climatic impacts of a collapse of the Atlantic thermohaline circulation, *Clim. Change*, *54*, 251–267.

Vellinga, M., and R. A. Wood (2007), Impacts of thermohaline circulation shutdown in the twenty-first century, *Clim. Change*, doi:110.1007/s10584-006-9146-y.

Weaver, A. J., O. A. Saenko, P. U. Clark, and J. X. Mitrovica (2003), Meltwater pulse 1a from Antarctica as a trigger of the Bølling-Allerød Warm Interval, *Science*, *299*, 1709–1713.

Wunsch, C. (2003), Determining pale oceanographic circulations, with emphasis on the Last Glacial Maximum, *Quat. Sci. Rev.*, *22*, 371–385.

Zickfeld, K., A. Levermann, H. M. Granger, S. Rahmstorf, T. Kuhlbrodt, and D. W. Keith (2007), Expert judgements on the response of the Atlantic meridional overturning circulation to climate change, *Clim. Change*, *82*, 235–265.

A. Levermann and J. Schewe, Earth System Analysis, Potsdam Institute for Climate Impact Research, Telegrafenberg A62, D-14473 Potsdam, Germany. (anders.levermann@pik-potsdam.de)

M. Montoya, Dpto. Astrofísica y Ciencias de la Atmósfera, Universidad Complutense, Madrid E-28040, Spain.